ChemComm

RSC Publishing

COMMUNICATION

View Article Online
View Journal | View Issue

Cite this: *Chem. Commun.*, 2013, **49**, 6882

Received 15th April 2013,
Accepted 6th June 2013

DOI: 10.1039/c3cc42769b

www.rsc.org/chemcomm

Novel expanded porphyrin sensitized solar cells using boryl oxasmaragdyrin as the sensitizer†

Sandeep B. Mane,[ab] Jyun-Yu Hu,[c] Yu-Cheng Chang,[c] Liyang Luo,*[d] Eric Wei-Guang Diau*[c] and Chen-Hsiung Hung*[a]

Oxasmaragdyrin boron complexes were prepared and applied in DSSCs. The HOMO–LUMO energy gap analyses and theoretical calculations revealed that these expanded porphyrins are ideal sensitizers for DSSCs. A device containing oxasmaragdyrin–BF_2 as the sensitizer achieves an energy conversion efficiency of 5.7%.

Dye-sensitized solar cells[1] (DSSCs) have emerged as promising candidates amongst the green energy sources due to their advantages such as low cost, high performance, and easy processing.[2] Although a lot of factors determine the efficiency of DSSCs, the light-harvesting properties of a photosensitizer remain utmost importance. Recently, Yella *et al.* reported a Zn(II) porphyrin with the D–π–A push–pull structure showing a remarkable power conversion efficiency of 12.3% when incorporated with an organic dye into the $[Co(bipy)_3]^{2+/3+}$-based electrolyte under AM 1.5G simulated sunlight.[3] It is projected that the accessibility of high efficiency near-infrared (NIR) and panchromatic dyes might further improve the efficiency of DSSCs. From the spectroscopic point of view, the expanded porphyrins offer a broad range of compounds with absorption energies down to infrared regions.[4] Expanded porphyrins with more than four pyrrole subunits in the porphyrinic macrocycle have been widely used in a variety of applications including anion and metal sensors,[5] NIR sensing dyes,[6] two-photon absorption (TPA) materials,[7] and photodynamic therapy[8] due to their increased cavity sizes and unique properties in association with extended π-conjugation. Although enormous literature is available on porphyrin-sensitized solar cells[9] and red-shifted absorption bands of expanded porphyrins match well with the demands for a low energy sensitizer, surprisingly an expanded porphyrin has never been used as the sensitizer for DSSCs. To uncover the potential of applying expanded porphyrins to DSSC studies, herein we report the syntheses and photophysical and photovoltaic properties of boron chelated oxasmaragdyrins, a class of aromatic core-modified expanded porphyrin with a 22 π-electron conjugation. The oxasmaragdyrin boron complexes **4a–4e** with structures depicted in Scheme 1 demonstrate panchromatic incident photon-to-current efficiencies (IPCEs), high short-circuit photocurrent densities (J_{sc}), and moderate-to-good overall efficiencies revealing an opportunity to develop expanded porphyrin-based highly efficient sensitizers for DSSCs.

The desired oxasmaragdyrin complexes **4a–4e** were prepared in four steps in decent yields under mild reaction conditions. Oxasmaragdyrin **1** was prepared from 3+2 condensation of *meso*-(4-methoxyphenyl)dipyrromethane and 16-oxatripyrrane in the presence of TFA as the acid catalyst.[10] The BF_2 chelated complex **2** was prepared by treating **1** with triethylamine and $BF_3{\cdot}OEt_2$ in CH_2Cl_2 at room temperature. The treatment of oxasmaragdyrin–BF_2 complex **2** with an excess amount of the corresponding alcohol in the presence of $AlCl_3$ at refluxing temperature for 10 min yielded dialkoxyboranyl chelated **3b–3e**.[11] The final oxasmaragdyrins **4a–4e** were isolated in moderate yields by hydrolysis of the precursors **2** and **3b–3e** with aqueous KOH in THF under reflux conditions (Scheme 1). In our design, alkoxy groups with long chains from C_2 to C_{10} were introduced to shield oxasmaragdyrins from aggregation and to increase their solubility.

The absorption spectra of oxasmaragdyrins **4a–4e** display split *Soret* bands in the 400–500 nm region and Q-bands in the 550–750 nm region as shown in Fig. 1. Markedly, the split *Soret* band covers a broader range of absorption wavelengths than regular porphyrins. Additionally, the Q-bands, which are more intense than

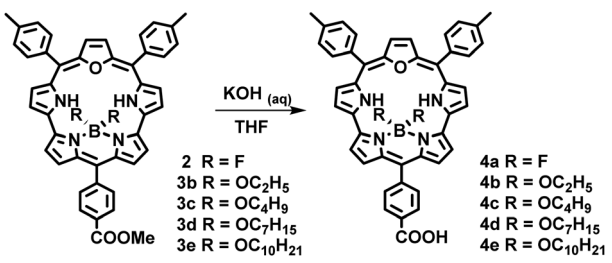

Scheme 1 Synthesis of boryl oxasmaragdyrins **4a–4e**.

[a] *Institute of Chemistry, Academia Sinica, Taipei 115, Taiwan. E-mail: chhung@gate.sinica.edu.tw; Tel: +886-2-27898570*

[b] *Department of Chemistry, National Taiwan Normal University, Taipei, 11677, Taiwan*

[c] *Department of Applied Chemistry and Institute of Molecular Science, National Chiao Tung University, Hsinchu 300, Taiwan. E-mail: diau@mail.nctu.edu.tw; Tel: +886-3-5131524*

[d] *Department of Chemistry, Chung Yuan Christian University, Chung Li, 32023, Taiwan*

† Electronic supplementary information (ESI) available. See DOI: 10.1039/c3cc42769b

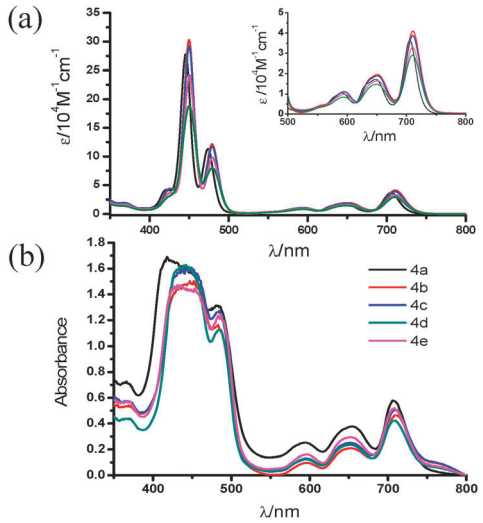

Fig. 1 Absorption spectra of oxasmaragdyrins **4a–4e**: (a) in THF (inset: expansion of Q-bands) and (b) adsorbed on TiO_2.

those for typical zinc or free base porphyrins and are mainly contributed from the HOMO to LUMO transition (Table S-1, ESI†), give the highest extinction coefficient (ε) at 710 nm, a shift of almost 100 nm in the NIR region compared to Zn(TPP).

The quantum-chemical calculations of structural optimization were performed for compounds **4a–4e** using the density functional theory (DFT) with the B3LYP functional and the 6-31G basis set. The results show planar structures for all studied dyes (see Fig. S-16, ESI†). Two alkoxide long chains lie on opposite sides of the oxasmaragdyrin plane and extend over to shield the furan ring. The calculations indicate that in the HOMO and HOMO − 1 orbitals, the majority of the electron density localizes on the macrocyclic π-system of the oxasmaragdyrin ring whereas in the LUMO and LUMO + 2 orbitals, electron densities delocalized further to the *meso*-carboxyphenyl anchoring group. The effective electron density redistribution should facilitate efficient electron injection from the excited state of oxasmaragdyrin to the conduction band of TiO_2. Significantly, theoretical calculations also revealed a higher molecular dipole moment (8.60 D) for the BF_2 chelated **4a** than an average of 7.86 D for $B(OR)_2$ chelated oxasmaragdyrins. The higher polarizability is beneficial to facilitate intramolecular photoinduced electron transfer. The cyclic voltammetry (CV) measurements of all oxasmaragdyrins **4a–4e** showed two reversible oxidation and one reversible reduction couples (Fig. S-15, ESI†). The static potentials and currents under multiple scans suggest high stability and reversibility of these compounds. The data in Table 1 show that the oxidation potentials of oxasmaragdyrins **4b–4e** shifted towards less positive by 140 to 170 mV resulting in elevated HOMO levels compared to oxasmaragdyrin–BF_2 **4a**. The reduction potentials of **4b–4e** shifted toward more negative by approximately 120 mV than that of the oxasmaragdyrin–BF_2 complex. Based on $E_{(0,0)}$ obtained from absorption and emission spectra and the first oxidation potential obtained from CV, the ground state oxidation potentials (E_{ox}) and excited state oxidation potentials (E_{ox}*) were calculated as listed in Table 1. For all of the oxasmaragdyrin boryl complexes, E_{ox}* are more negative than the conduction band edge of the TiO_2 electrode while the E_{ox} are more positive than the redox potential of I^-/I_3^-. Although the red-shift in the absorption band of

Table 1 Photophysical and electrochemical data for oxasmaragdyrin dyes

Dye	λ_{abs} [a] [nm] (ε [10^3 M^{-1} cm^{-1}])	E_{ox} [b] [V]	$E_{(0,0)}$ [c] [eV]	E_{ox}* [d] [V]
4a	446 (278), 474 (113), 706 (36)	0.86	1.75	−0.89
4b	450 (303), 479 (121), 711 (41)	0.69	1.73	−1.04
4c	450 (291), 479 (117), 711 (38)	0.71	1.73	−1.02
4d	450 (242), 480 (98), 710 (32)	0.72	1.73	−1.01
4e	450 (188), 480 (79), 710 (29)	0.71	1.73	−1.02

[a] In THF. [b] First oxidation potentials *vs.* NHE in THF calibrated by the Fc/Fc^+ couple. [c] Estimated from the intersection of the absorption and emission spectra. [d] Approximated from E_{ox} and $E_{(0,0)}$.

oxasmaragdyrins indicated a smaller band gap between HOMO and LUMO levels, the electrochemical data confirm the high driving force for both electron injection and dye regeneration.

The BF_2 and $B(OR)_2$ chelated oxasmaragdyrins **4a–4e** were fabricated into the solar cell devices in the presence of CDCA as a co-adsorbent as detailed in the ESI.† [12] Fig. 2a shows the current–voltage plots of the devices measured under standard AM 1.5G simulated solar conditions; the photovoltaic parameters are summarized in Table 2. The DSSCs sensitized with oxasmaragdyrin–BF_2 complex **4a** exhibited the best performance with a short-circuit photocurrent density (J_{sc}/mA cm^{-2}) of 13.71, an open-circuit voltage (V_{oc}/V) of 0.591, and a fill factor (FF) of 0.703, corresponding to an overall power conversion efficiency (η) of 5.70%. The oxasmaragdyrin derivatives **4b–4e** all had efficiencies lower than that of the BF_2 complex **4a**, with a typical trend of an improved device performance upon increasing the length of alkoxy chains. The trend of J_{sc} in this series can be understood from the variation of IPCE action spectra shown in Fig. 2b. The lower efficiencies of devices **4b** and **4c** can be partly attributed to the lower dye-loading (DL) as shown in Table 2. We noted that the IPCE values corresponding to the absorption region of the *Soret* band of device **4a** reached 60%, and those of the Q band were around 50%. Also the dip between 500 and 600 nm was much higher (around 40%) for device **4a** compared to the devices **4b–4e**. To understand the key factors accounting for the IPCE values observed herein, we carried out transient photoelectric and charge-extraction (CE) measurements for the five devices under investigation.

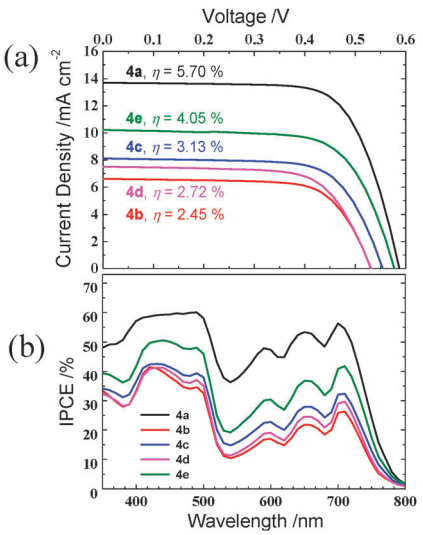

Fig. 2 (a) *I–V* characteristics and (b) IPCE spectra of DSSCs fabricated with oxasmaragdyrins **4a–4e** under 100% sun (AM 1.5G).

Table 2 Photovoltaic properties of devices with **4a–4e** dyes[a]

Dye	DL [nmol cm^{-2}]	J_{sc} [mA cm^{-2}]	V_{oc} [V]	FF [%]	η [%]
4a	184	13.71	0.591	703	5.70
4b	110	6.60	0.535	695	2.45
4c	119	8.12	0.558	690	3.13
4d	146	7.51	0.534	679	2.72
4e	194	10.22	0.581	682	4.05

[a] Immersion in EtOH at room temperature for 6–8 h.

The charge densities (N_e) of the devices under a certain bias light irradiation and open-circuit conditions were determined *via* CE measurements when the circuit of the system was switched to the short-circuit conditions.[13] The CE results show that the extracted charge densities were much smaller than those of highly efficient devices reported elsewhere,[13] indicating that either less electrons were injected into the conduction band of TiO_2, or the system involved a serious problem in expediting the charge recombination at the dye/TiO_2 interface. As a result, transient photovoltage decay (ΔV_{oc} *vs.* time) was performed using the small-amplitude approach based on seven white-light intensities (power densities in the range 7–102 mW cm^{-2}) as bias irradiation under open-circuit conditions.[13] Decay curves of ΔV_{oc} *vs.* time for the five devices were fitted according to a single exponential function to determine time coefficients for charge recombination (τ_R). Fig. 3a and b show the plots of τ_R *vs.* N_e and V_{oc} *vs.* N_e, respectively. The plots of V_{oc} *vs.* N_e show that the potentials were down-shifted upon increasing the length of the alkoxyl chains, and this trend is against the variation of V_{oc} showing the opposite trend (Table 2). On the other hand, we found that the values of τ_R in this series are much smaller than those reported for highly efficient dyes,[13] confirming that the relatively poor device performances of these porphyrins are due to the effect of rapid charge recombination. This effect causes significant reduction of the charge densities in the conduction band of TiO_2, and thus leads to a decrease in the performance for both J_{sc} and V_{oc}. The plots of τ_R *vs.* N_e shown in Fig. 3a display a systematic trend of τ_R for $B(OR)_2$ complexes with **4e** > **4c** > **4d** > **4b**, consistent with the variation of V_{oc} in this series. These results indicate that the two alkoxyl chains attached to the boron center could help in retarding the charge recombination. Typically, a longer alkoxyl chain would have a better retardation effect to repel the approach of triiodide anion species toward the surface of TiO_2 for a larger τ_R and a higher V_{oc}, but an exception for the **4d** complex with heptoxyl chains was observed. Interestingly, we observed that the τ_R values of **4e** were significantly greater than those of **4a**, which cannot explain the fact that V_{oc} of **4a** was slightly larger than that of **4e**. We expect that the electron injection efficiency of the **4a** device should be greater than that of the **4e** device so as to generate more injected electrons in the CB of TiO_2 to give a larger Fermi level for the observed higher V_{oc} for the former than for the latter. The effect of electron injection can also be applied to rationalize the observed trend of J_{sc}, which is higher for **4a** than for **4e**.[14]

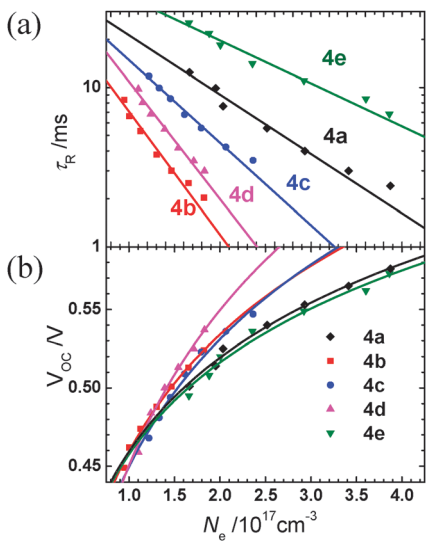

Fig. 3 Plots of (a) charge recombination time coefficient (τ_R) *vs.* electron density (N_e) and (b) V_{oc} *vs.* N_e for DSSCs fabricated with **4a–4e**.

In conclusion, we were able to demonstrate for the first time that boron complexes of oxasmaragdyrin, a class of core-modified expanded porphyrin, can be applied as efficient photosensitizers for DSSC. In contrast to the relatively low efficiencies of the devices using BODIPY derivatives as the sensitizers,[15] boron chelated oxasmaragdyrins provide desired redox potentials, high absorption coefficients, high stability, and higher power conversion efficiencies suitable for an effective sensitizer in DSSCs. More importantly, broad absorption spreading over the entire visible region and its lower energy Q band covering part of the NIR region make this class of compound an optimistic candidate for being one of the future selections of porphyrin-sensitized solar cells.

Notes and references

1 B. O'Regan and M. Gratzel, *Nature*, 1991, **353**, 737.
2 (*a*) L. M. Goncalves, V. de Zea Bermudez, H. A. Ribeiro and A. M. Mendes, *Energy Environ. Sci.*, 2008, **1**, 655; (*b*) Y. Luo, D. Li and Q. Meng, *Adv. Mater.*, 2009, **21**, 4647; (*c*) M. Grätzel, *Acc. Chem. Res.*, 2009, **42**, 1788; (*d*) A. Hagfeldt, G. Boschloo, L. Sun, L. Kloo and H. Pettersson, *Chem. Rev.*, 2010, **110**, 6595.
3 A. Yella, H.-W. Lee, H. N. Tsao, C. Yi, A. K. Chandiran, M. K. Nazeeruddin, E. W.-G. Diau, C.-Y. Yeh, S. M. Zakeeruddin and M. Grätzel, *Science*, 2011, **334**, 629.
4 J. M. Lim, Z. S. Yoon, J.-Y. Shin, K. S. Kim, M.-C. Yoon and D. Kim, *Chem. Commun.*, 2009, 261.
5 (*a*) B. Sridevi, S. J. Narayanan, R. Rao, T. K. Chandrashekar, U. Englich and K. Ruhlandt-Senge, *Inorg. Chem.*, 2000, **39**, 3669; (*b*) J. L. Sessler, S. Camiolo and P. A. Gale, *Coord. Chem. Rev.*, 2003, **240**, 17; (*c*) Y. Ikawa, M. Takeda, M. Suzuki, A. Osuka and H. Furuta, *Chem. Commun.*, 2010, **46**, 5689.
6 K. Naoda, H. Mori, N. Aratani, B. S. Lee, D. Kim and A. Osuka, *Angew. Chem., Int. Ed.*, 2012, **51**, 9856.
7 R. Misra, R. Kumar, T. K. Chandrashekar, C. H. Suresh, A. Nag and D. Goswami, *J. Am. Chem. Soc.*, 2006, **128**, 16083.
8 (*a*) S. K. Pushpan, V. G. Anand, S. Venkatraman, J. Sankar, D. Parmeswaran, S. Ganesan and T. K. Chandrashekar, *Curr. Med. Chem.: Anti-Cancer Agents*, 2002, **2**, 187; (*b*) J. Seenisamy, S. Bashyam, V. Gokhale, H. Vankayalapati, D. Sun, A. Siddiqui-Jain, N. Streiner, K. Shin-ya, E. White, W. D. Wilson and L. H. Hurley, *J. Am. Chem. Soc.*, 2005, **127**, 2944.
9 L.-L. Li and E. W.-G. Diau, *Chem. Soc. Rev.*, 2013, **42**, 291.
10 S. J. Narayanan, B. Sridevi, T. K. Chandrashekar, U. Englich and K. Ruhlandt-Senge, *Org. Lett.*, 1999, **1**, 587.
11 M. Rajeswara Rao and M. Ravikanth, *J. Org. Chem.*, 2011, **76**, 3582.
12 Y. Li, P. Lu, X. Yan, L. Jin and Z. Peng, *RCS Adv.*, 2013, **3**, 545.
13 L.-L. Li, Y.-C. Chang, H.-P. Wu and E. W.-G. Diau, *Int. Rev. Phys. Chem.*, 2012, **31**, 420.
14 C. Y. Lee, C. She, N. C. Jeong and J. T. Hupp, *Chem. Commun.*, 2010, **46**, 6090.
15 S. Kolemen, O. A. Bozdemir, Y. Cakmak, G. Barin, S. Erten-Ela, M. Marszalek, J.-H. Yum, S. M. Zakeeruddin, M. K. Nazeeruddin, M. Gratzel and E. U. Akkaya, *Chem. Sci.*, 2011, **2**, 949.

